Effects of Aging Conditions on Fracture Characteristics of Al–Mg–Si Alloys

Zeynep Tutku Özen, İlyas Artunç Sarı, Anıl Umut Özdemir, Abdullah Kağan Kınacı, Emre Çankaya, Alptuğ Tanses, and Görkem Özçelik

Abstract

The automotive industry has started using lightweight materials like aluminum with the aim of increasing fuel efficiency by supporting carbon neutral production. Structural parts of an automobile like bumper and chassis requires not only tensile strength but also crashworthiness. One of the main requirements of an aluminum alloy is to increase crashworthiness by over aging of the alloys. In this study, 6005 aluminum alloy production has been followed with automotive parts production route of billet production by direct chill casting, homogenization, extrusion and heat treatment. Different natural and artificial aging conditions have been applied to 6005 alloy. Strengths, crashworthiness, elongations and fracture characteristics have been evaluated according to the results of characterization studies including tensile tests and SEM Analysis.

Keywords

Aluminum • Billet casting • Extrusion • Crashworthiness • 6005 alloy

Introduction

Aluminum alloys are preferred for several usage areas due to their low density, high specific strength and corrosion resistance. One of the main usage areas of aluminum alloys is automotive industry with respect to performance, safety, fuel efficiency, durability and environmental benefits. When safety issues are considered, aluminum has high crashworthiness as it is able to absorb twice as much energy than the same weight of steel. This feature of aluminum enables it to be used for the manufacturing of front and back crumple zones of a vehicle [1, 2].

Aluminum extrusion is a process which produces aluminum profiles. In order to produce profiles, an extrusion equipment applies force to the billet material which has previously heated, causing plastic deformation of the material. The mentioned deformation of the pre-heated billets occurs in an extrusion die which has crucial parts such as bolster, bracket and dummy block to sustain the required force. As a result of billet motion and the applied force of the extrusion press, production of certain cross-sectioned profiles is possible. Aluminum profiles are preferred in structural applications to produce parts for automotive, railway, aerospace and architecture sectors. The technology that enables the production of closed sections in different thickness values is an integral part of the mass production of automotive parts [2, 3].

Figure 1 shows the aluminum alloys mainly used in different parts of the cars as a component [10]. Main aluminum alloys are 5xxx and 6xxx series Body-in-White parts production. Table 1 shows the aluminum alloys and their main usage areas for the automotive industry, with respect to their properties have been summarized. Generally processing of different wrought alloys is different as well. 1xxx, 3xxx, 5xxx alloys are generally cold rolled, 2xxx, 6xxx and 7xxx alloys are generally extruded, 4xxx alloys are generally pressure casted and some 5xxx and 6xxx alloys may be hot rolled [3–7].

In order to produce a crash management system for an automobile, 6xxx series aluminum alloys are used mainly since they have properties like high compression strength, moderate tensile strength and good impact resistance. Also, design optimization freedom of the extrusion process makes extrusion a good manufacturing method for lightweight constructions. Also, 6xxx alloys have good formability which is desired with respect to extrusion process. Especially, 6005 and 6063 alloy are used for crash management

Z. T. Özen (✉) · İ.A. Sarı · A. U. Özdemir · A. K. Kınacı · E. Çankaya · A. Tanses · G. Özçelik
ASAŞ Aluminium San. Ve Tic. A. Ş, Sakarya, Turkey
e-mail: tutku.ozen@asastr.com

S. Broek (ed.), *Light Metals 2023*, The Minerals, Metals & Materials Series,
https://doi.org/10.1007/978-3-031-22532-1_39

Fig. 1 Different materials used in vehicles [10]

Table 1 Usage areas of wrought aluminum alloys for automotive industry [5–7]

Aluminum alloy	Components of car	Features
1xxx	Heat insulators	Excellent corrosion resistance
2xxx	Pistons, break components, rotors, cylinders, wheels, gears	High strength, high fatigue resistance
3xxx	Piping, paneling, radiators, body sheet, fenders, doors, floor paneling	Good formability, good workability, good drawing characteristics, excellent corrosion resistance,
4xxx	Pistons, compressor scrolls, engine components	Excellent weldability, abrasion resistance, good castability
5xxx	Body paneling, fuel tanks, steering plates, piping, disk and drum breaks	Highest strength of non-heat treatable alloys. readily weldable
6xxx	Cross members, brakes, wheels propeller shafts, truck and bus bodies, crashbox	Dent resistance, excellent surface finishing characteristics, corrosion resistance, high strength, impact resistance
7xxx	Impact beams, seat sliders, bumper reinforcement, motorbike frames, rims	Highest strength, good welding character

systems as a crash box material due to their compression behaviors under stress. The decision on aluminum alloys for crash box production is done with respect to the final usage area and process efficiency approaches. One of the main variables that affects properties of these alloys is heat treatment process and its efficiency. In this study, the effects of natural aging caused by industrial delays of the profiles to be heat treated and different artificial aging durations have been investigated to increase process efficiency with respect to the results [3, 4].

Study Flowchart

In this study, the process has begun with the direct chill casting of 14 inches (355 mm) billets of 6005 aluminum alloys in the prototype casting facility of ASAS Aluminum. After the casting operation, chemical spectrometer analysis of the billets has been done via mass spectrometer. Compositions of the casted alloy have been shown at the Table 2 with its related standard.

Table 2 Chemical composition of 6005 alloys

	Si	Fe	Cu	Mn	Mg	Zn	Cr	Ti
EN 573-3	0.5–0.9	0–0.35	0–0.3	0–0.5	0.4–0.7	0–0.2	0–0.3	0–0.1
ASAS	0.65	0.3	0.1	0.1	0.5	0.1	0.1	0.1

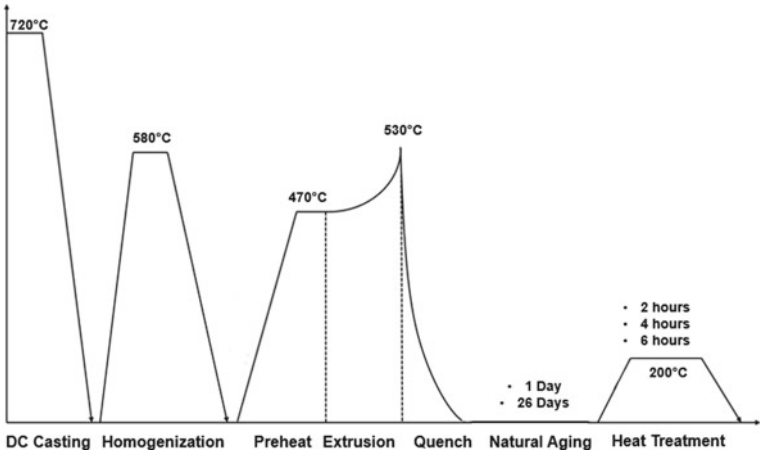

Fig. 2 Flowchart of this study

Table 3 Experimental design of the study

	AA6005—200 °C—2 h	AA6005—200 °C—4 h	AA6005—200 °C—6 h
Profiles in 1 day	Tensile test, compression test, fractography	Tensile test, compression test, fractography	Tensile test, compression test, fractography
Profiles in 26 day	Tensile test, compression test, fractography	Tensile test, compression test, fractography	Tensile test, compression test, fractography

Billets were homogenized in a batch type homogenization furnace at 580 °C for 3 h. The extrusion process has been carried out in an extrusion press with 29 MN force capability. The inlet temperature of the extrusion is 470 °C and the outlet temperature is 530 °C. The procedure was followed by quenching through water spraying at 80% capacity. Following the quench, 1.4% stretching was applied and profiles were cut into requested the length of 2250 mm. Natural aging is applied to the profiles for 1 day and 26 days separately. Artificial aging studies are carried out to both naturally aged and non-aged profiles at the temperature of 200 °C with the duration of 2, 4 and 6 h. The flowchart of this study can be seen in Fig. 2.

Characterization and test are carried out after the production route. Compression tests are carried out with a 160 tons hydraulic press. Tensile tests are applied with a Zwick universal testing device. Analysis of fracture types has been carried out with fractured tensile test specimens via SEM, Zeiss EVO MA15 brand. Table 3 demonstrates the design of the experiments respectively.

Results and Discussion

Results of this study have been investigated with respect to mechanical properties, crash properties and fracture characteristics of the alloys with different aging conditions.

Figures 3 and 4 illustrate the effects of applying prolonged natural pre-aging (NA) and subsequent three different artificial aging (AA) durations on mechanical properties. In general, there is a decreasing trend in yield and tensile strength after conducting NA and AA. The yield strength of the NA 1 day and AA 2 h at 200 °C sample is 275 MPa and the tensile strength of it is 298 MPa, respectively. On the other hand, when the NA time is increased to 26 days and the same AA condition is applied, the yield tensile strength decreased to 267 MPa. The tensile strength difference of naturally aged sample at 2 h of artificial aging conditions is very slight with 295 MPa. The yield strength of NA 1 Day and AA 4 h at 200 °C sample is 272 MPa its tensile strength is 296 MPa. Same AA conditions results in a higher

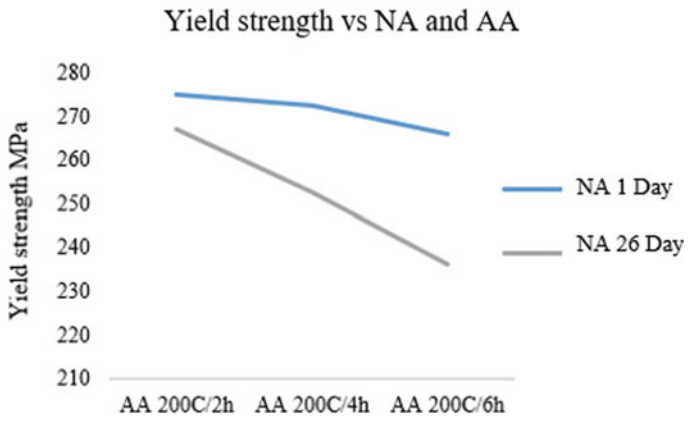

Fig. 3 Yield strength curve of naturally and artificially aged profiles

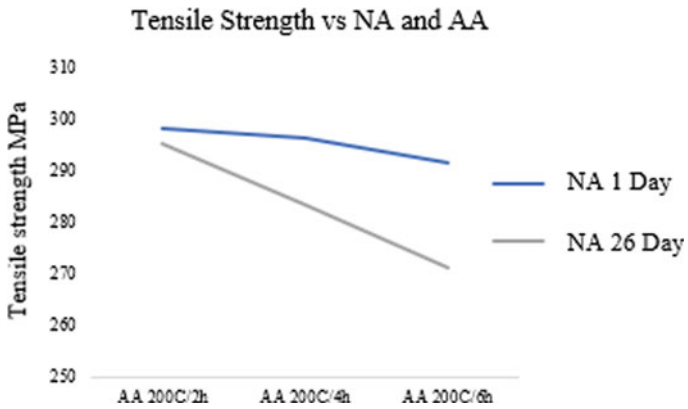

Fig. 4 Tensile strength curve of naturally and artificially aged profiles

decrease for naturally over aged samples. Yield strength of it is 252 MPa and the tensile strength of it is 283 MPa. Finally, AA 6 h condition results in 266 MPa yield strength and 291 MPa tensile strength for NA 1-day samples and 236 MPa yield strength and 271 MPA tensile strength for NA 26 days samples. As a result, both yield and tensile strength values have been decreased with increasing aging time and with the presence of natural aging. Also, yield strength of minimum duration artificially aged and naturally aged samples shows similar mechanical properties with 6 h of artificial aged and non-naturally aged samples. Thus, natural aging conditions affect negatively the mechanical properties of 6005 alloys. One can claim that, 26 days of natural aging has similar mechanical properties to 6 h artificial aging at 200 °C.

When the AA time is increased from 2 to 4 h at the same AA temperature, yield strength has decreased by approximately 1% and the tensile strength around 0.5% for NA 1 day. These ratios increased to 5.5% yield difference and 4% tensile strength difference at NA 26 days. While evaluating decrease of the strength with respect to artificial aging duration both for naturally aged and non-aged samples from 4 to 6 h, non-aged samples showed 2% decrease for yield strength and 2% decrease for tensile strength. Naturally aged samples values are 6% decrease for yield strength and 4% decrease for tensile strength respectively.

As long as NA is prolonged the effect of AA increases significantly on mechanical properties. The effects of longer NA might be due to the accumulation of β″ precipitates as the natural aging time increases. Besides, dissolution kinetics of these clusters and the growth of β″ needles slows down at subsequent AA [8].

Figures 5, 6, 7, 8, 9 and 10 illustrate the SEM images of tensile fracture morphology of artificial aging specimens with different natural aging durations. Secondary electron (SE) images have been taken to observe shapes of dimples. Also, frequency of the dimples has been analyzed respectively. Backscattered electron images (BSE) have been taken to interpret fracture characteristics with respect to depth of dimples. Finally, the numbers, distributions and morphologies of dispersoids have been investigated with × 3000 magnified BSE Images of fractured surfaces. As a general observation for all specimens, the width of dimples is reduced while the depth and density of the dimples are increased as exposed to longer natural aging.

According to Fig. 5a, frequency of the dimples is lower than others. Also, dimension of the dimples relatively higher. This is caused because of the relatively lower

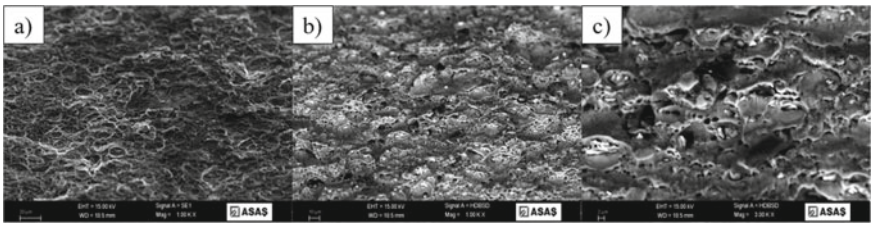

Fig. 5 SEM images of 1 day NA and 2 h AA at 200 °C specimens; **a** SE image with 1000 ×magnification, **b** BSE image with 1000 ×magnification, **c** BSE image with 3000 × magnification

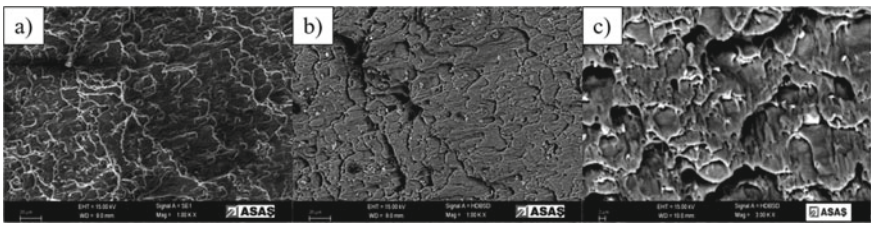

Fig. 6 SEM images of 1 day NA and 4 h AA at 200 °C specimens; **a** SE image with 1000 × magnification, **b** BSE image with 1000 × magnification, **c** BSE image with 3000 × magnification

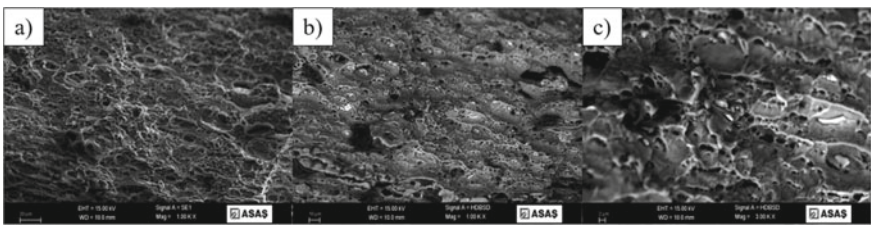

Fig. 7 SEM images of 1 day NA and 6 h AA at 200 °C specimens; **a** SE image with 1000 × magnification, **b** BSE image with 1000 × magnification, **c** BSE image with 3000 × magnification

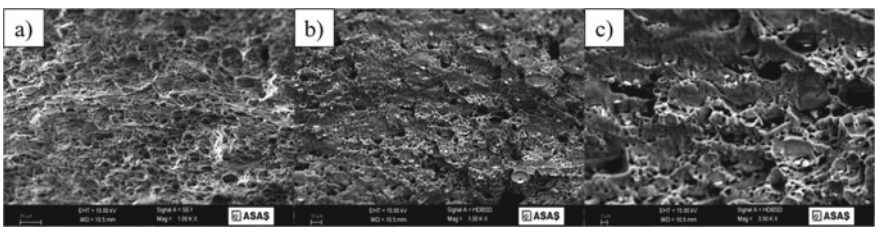

Fig. 8 SEM images of 26 Day NA and 2 h AA at 200 °C specimens; **a** SE image with 1000 × magnification, **b** BSE image with 1000 × magnification, **c** BSE image with 3000 × magnification

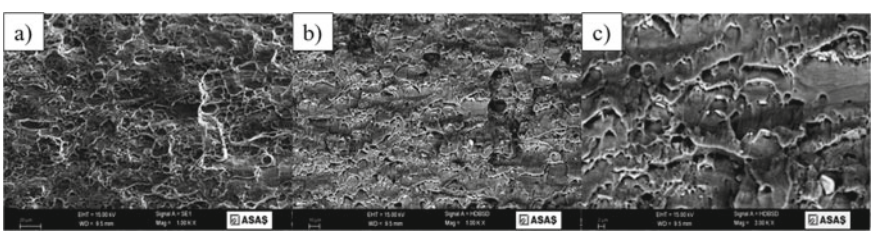

Fig. 9 SEM images of 26 day NA and 4 h AA at 200 °C specimens; **a** SE image with 1000 × magnification, **b** BSE image with 1000 × magnification, **c** BSE image with 3000 × magnification

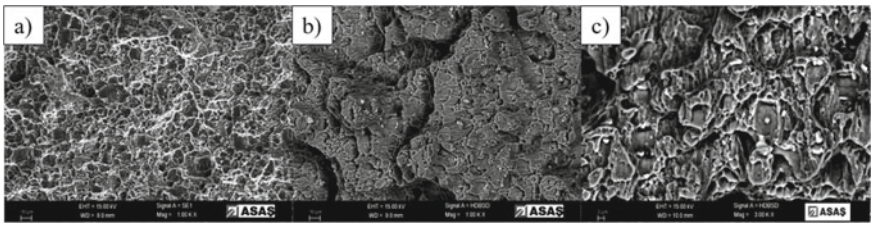

Fig. 10 SEM images of 26 day NA and 6 h AA at 200 °C specimens; **a** SE image with 1000 × magnification, **b** BSE image with 1000 × magnification, **c** BSE image with 3000 × magnification

ductility of the material. Shapes of the dimples are generally rounded. Figure 5b shows the BSE images with × 1000 magnification. Depths of the dimples are low which supports the brittle fracture characteristics and mechanical properties. Figure 5c, shows the dispersoids shape and distribution. The dispersoids located at the edges of the dimples and they have round and spherical shapes. It can be stated that, fracture caused mainly around dispersoids.

Figure 6a demonstrates the SE Images of 1 Day NA and 4 h AA specimens. The frequency of the dimples is lower than others. Also, the size of the dimples is relatively higher. This is because of the relatively lower ductility of the material. However, it should be in between of 2 and 6 h results. There should be surface abrasion caused from laboratory conditions. Shapes of the dimples are generally rounded for this investigation. BSE images with × 1000 magnification has been showed at the Fig. 6b. Depths of the dimples are higher than 2 h artificially aged samples and lower than 6 h aged samples which supports the mechanical properties. Figure 6c, shows the dispersoids shape and distribution. The dispersoids located at the edges of the dimples and they have more sharp edges than 2 h aged specimens.

The most ductile fracture characteristic is observed for 1 day naturally aged samples as shown in Fig. 7a. The frequency of the dimples is higher than others. Also, dimension of the dimples is relatively lower. Shapes of the dimples are generally rounded for this investigation. Depths of the dimples are higher than other non-naturally aged samples with respect to Fig. 7b. Shapes of the dispersoids have needle like structure which has been illustrated at Fig. 7c.

Figure 8a illustrates the dimples shape and distribution for 26 days naturally aged and 2 h artificially aged samples. The sizes of the dimples are lower than non-naturally aged ones but higher than naturally aged and 6 h artificially aged samples. The fracture characteristic has similar topology with 1 day naturally aged and 6 h artificially aged samples. The depth of the dimples are higher than other 2 h AA sample but lower than 26 days NA and 6 h AA samples which is shown in Fig. 8b. Dispersoid shapes are rounded as it is demonstrated at Fig. 8c. This can be caused by the effect of natural aging on intermetallic precipitates growth.

Figure 9a shows the SE image of 26 days NA and 4 h at 200 °C AA samples with × 1000 magnification. As it can be observed, frequency of dimples is higher than others and the size of them lower than the others. This results also supports the ductile fracture and low strength values. Depths of the dimples are higher than the other specimens except the one with 26 days NA and 6 h AA. This can be seen from the Fig. 9b. Dispersoids have more sharp edges than the samples with 26 days NA and 2 h AA. The shapes of these dispersoids are illustrated at the Fig. 9c.

Figure 10a demonstrated the most ductile fracture behavior of all with highest frequency of dimples and lowest sizes of them. Results are supporting the increased aging conditions for aluminum alloys yields in increasing the ductility and decreased strength phenomena. The deepest fracture dimples are observed at the Fig. 10b which is belong to 26 days NA and 6 h AA at 200 °C samples. Surprisingly, dispersoids are spherical and located at the middle of dimples. This situation can be seen in Fig. 10c. The reason why dispersoids have greater size and rounded shape is the over aging conditions with respect to study of Alexopoulos et al. [9].

Conclusion

In this work, effects of natural aging and different artificial aging conditions on mechanical properties of 6005 aluminum alloys are studied. As a general result, natural aging has negative effects on strength values of the 6005 alloys, the strength also decreases when artificial aging time increases to 4 h at 200 °C and more. It can be claimed that 4 h and 6 h samples are over-aged. Furthermore, it can be stated that samples with a 26 days natural aging duration and 2 h artificial aging at 200 °C has similar mechanical properties with 1-day natural aging duration (non-naturally aged) and 6 h at 200 °C artificially aged samples. According to SEM results, existence of dimples demonstrates that the fracture type is ductile. Increased dimple frequency and small size of dimples refer to enhanced ductile behavior on the other hand the lesser frequency and bigger dimples refer to lower

ductile behavior compared to the higher frequency and smaller size dimple containing material. The opposite situation where dimples are bigger and their frequencies are lower, implies that the strength of the material is higher. In this study, non-naturally aged and 2 h AA samples showed highest strength with brittle fracture characteristics. The samples with 26 days NA and 6 h AA showed a great example for over-aging where dispersoids are agglomerated and showed spherical behavior in the middle of the dimples. Investigation of crash properties and natural aging mechanism would be fruitful for further research.

References

1. Mallick, P. K., & Graf, A. (2010). Aluminum alloys for lightweight automotive structures. In Materials, design and manufacturing for Lightweight Vehicles (pp. 97–123). Essay, CRC Press.
2. Miller, W. S., Zhuang, L., Bottema, J., Wittebrood, A. J., De Smet, P., Haszler, A., & Vieregge, A. (200). Recent development in aluminium alloys for the automotive industry. Materials Science and Engineering: A, 280(1), 37–49. https://doi.org/10.1016/s0921-5093(99)00653-x
3. Lakshmi, A., Buddi, T., Subbiah, R., & Bandhavi, C. (2020). Formability studies of Automotive Aluminium Alloy Sheet Series: A Review. E3S Web of Conferences, 184, 01036. https://doi.org/10.1051/e3sconf/202018401036
4. Konar, M., Aslanlar, S., İlhan, E., Kekik, M., Özçelik, G., Güner, M. B., Yiğit, A. F., & Demirkıran, T. (2021). Investigation of weld quality for friction stir welding of extrued 6xxx series aluminium alloys. The Minerals, Metals & Materials Series, 220–226. https://doi.org/10.1007/978-3-030-65396-5_32
5. Sudhanwa M. Kulkarni, Priyal Vemu, Kiran D. Mali, Dhananjay M. Kulkarni, Effect of geometric irregularities induced during manufacturing of a crash-box on its crashworthiness performance, Materials Today: Proceedings, Volume 57, Part 2, 2022, Pages 715–721, ISSN 2214–7853, https://doi.org/10.1016/j.matpr.2022.02.179.
6. Montijo, S. (2022, September). Aluminum in cars: What aluminum alloys are common in aluminum car bodies? Kloeckner Metals Corporation. Retrieved September, 2022, from https://www.kloecknermetals.com/blog/aluminum-in-cars/
7. Understanding the alloys of aluminum. (n.d.). Retrieved September 2022, from http://www.alcotec.com/us/en/education/knowledge/techknowledge/understanding-the-alloys-of-aluminum.cfm#:~:text=5xxx%20Series%20Alloys%20%E2%80%93%20(non%2D,the%20non%2Dheat%20treatable%20alloys.
8. DING, X.-fei, SUN, J., YING, J., ZHANG, W.-dong, MA, J.-jun, & WANG, L.-chen. (2012). Influences of aging temperature and time on microstructure and mechanical properties of 6005a aluminum alloy extrusions. Transactions of Nonferrous Metals Society of China, 22. https://doi.org/10.1016/s1003-6326(12)61677-x
9. [9] Zhang, L., He, H., Li, S., Wu, X., & Li, L. (2018). Dynamic compression behavior of 6005 aluminum alloy aged at elevated temperatures. Vacuum, 155, 604–611. https://doi.org/https://doi.org/10.1016/j.vacuum.2018.06.066
10. Audi A3 - materials in the body structure. Car Body Design. (n.d.). Retrieved October 2022, from https://www.carbodydesign.com/gallery/2012/05/audi-a3-design-story/37/